PCCP

Accepted Manuscript

ROYAL SOCIETY OF CHEMISTRY

www.rsc.org/pccp

Journal Name

COMMUNICATION

An approach to the electronic structure of molecular junctions with metal clusters of atomic thickness†

Received 00th January 20xx,
Accepted 00th January 20xx

DOI: 10.1039/x0xx00000x

www.rsc.org/

Daniel Aranda, Isabel López-Tocón, Juan Soto, Juan C. Otero* and Francisco Avila*

TD-DFT calculations predict a linear dependence of the energies of charge transfer states of Ag_n-pyrazine-Ag_n molecular junctions on the inverse of the size (1/n) of the linear metal chains. The density of charge (q_{eff}=q/n) in the metal-to-metal charge transfer excited states (CT_{MM}:Ag_n^q-pyrazine-Ag_n^{-q}) tunes smoothly the electronic structure of the junction, especially the metal-to-molecule charge transfer states (CT_0 and CT_1) and the first excited singlet of pyrazine ($S_{1,Pz}$). In enlarged junctions, pyrazine bonds preferably to one of the Ag_n clusters and this weak adsorption produces a significant unexpected asymmetry for forward and reverse charge transfer processes.

A deep understanding of the electronic transport through molecular junctions is the key for the development of molecular electronics.[1,2] Molecular junctions consist in a single molecule (A) placed between two metallic electrodes (M_n) where the transmission event can be non-resonant or resonant if metal-to-molecule (M^+-A^-) or molecule-to-metal (A^+-M^-) charge transfer states (CT) or excited states of the molecule (A*) are intermediate steps in the conduction. In this case, the conductance undergoes a dramatic enhancement and the electronic structure of the molecule and its chemical anchoring to the metal electrodes control the electric transport. A resonant conduction channel can be enabled if these metal-molecule or molecular states lie inside the window between the Fermi levels (FL's) of both metals in the case of large conductors, or between the corresponding $HOMO_M$ and $LUMO_{M'}$ orbitals of small insulating or semiconductor metal clusters. But the relative energies of these states are tuned in a complex way by the applied electric potential (E_V) making necessary the use of simplified schemes like shown Fig. 1a, where E_V shifts only both FL's with respect to the energies of the $HOMO_A$ and $LUMO_A$ orbitals of the molecule which remain unaltered. Subtle chemical contributions are missing in these schemes and the complex dependence of the electronic states of the overall M-A-M' system on the applied bias is not taken into account.

In this work a strategy based on time-dependent DFT calculations (TD-DFT) to model the effect of the size, the density of charge and the inter-cluster distance on the overall electronic structure of molecular junctions containing two silver nanowires with monoatomic thickness is introduced. A very symmetric D_{2h} molecule (pyrazine, Pz) has been selected which is N-linked to the electrodes (Fig. 2). Nowadays scanning tunnelling microscopy techniques are able to build these molecular junctions with linear chains of noble metal atoms and to carry out spectroscopic measurements.[3-5] Pz molecule is placed between the two silver linear clusters in a planar collinear configuration Ag_n-Pz-Ag_n, with n=2,4,6 and 8, in order to study the effect of the metal cluster size in the electronic structure of the junction (Fig. 2). Guidez and Aikens[6,7] have reported TD-DFT calculations on the effect of the size on the electronic structure of single silver and gold atomic nanowires. In this work, these systems have been extended by adding a second metal chain and an organic molecule which connects both metal clusters. This allows for studying metal-to-metal and metal-to-molecule CT states as well as electronic

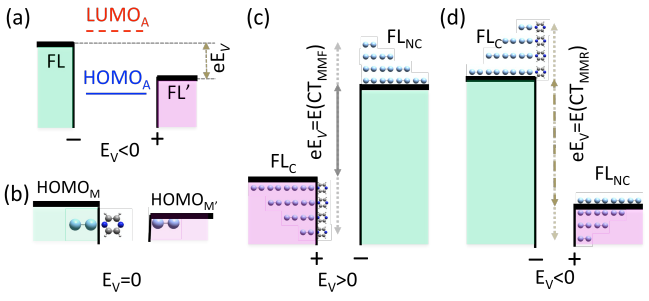

Fig. 1 (a) Usual scheme showing the effect of the applied bias (E_V) in the relative energies of the Fermi levels (FL) of the electrodes with respect to the $HOMO_A$ and $LUMO_A$ orbitals of the molecule. (b) Shift of the $HOMO_M$ induced by the molecular adsorption. (c,d) Fermi levels under positive or negative electrode potentials related to the metal-to-metal forward (CT_{MMF}) and reverse (CT_{MMR}) charge transfer states of Ag_n-Py-Ag_n with different sizes.

Universidad de Málaga, Andalucía Tech, Facultad de Ciencias, Departamento de Química Física, Unidad Asociada CSIC, 29071-Málaga, Spain. E-mail: jc_otero@uma.es, avila@uma.es

† Electronic supplementary information (ESI) available: See DOI: 10.1039/x0xx00000x

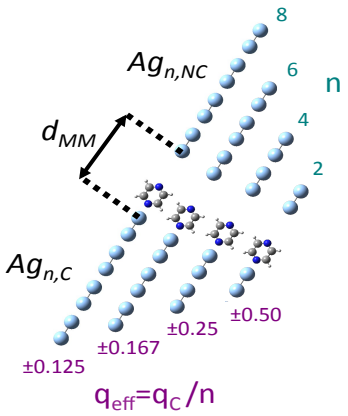

Fig. 2 Structures of Ag_n-Pyrazine-Ag_n molecular junctions and the corresponding effective density of charges ($q_{eff}= q_C/n$) of the contact metal electrode in the forward (q_C=+1) and reverse (q_C=-1) metal-to-metal CT_{MM} charge transfer states.

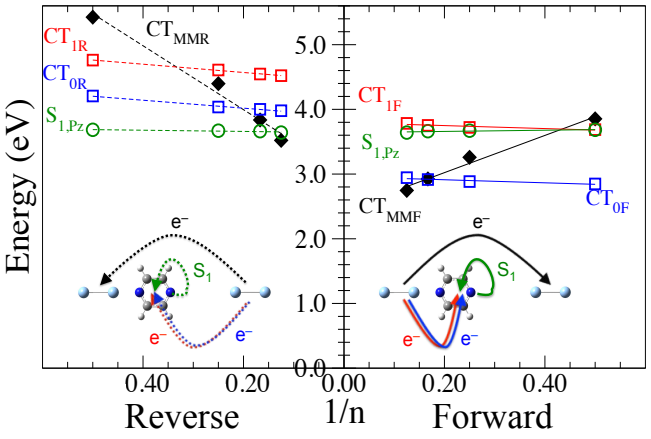

Fig. 3 M06-HF/LanL2DZ vertical excitation energies of metal-metal CT_{MM}, metal-molecule $CT_{0,1}$ and molecular $S_{1;Pz}$ states with respect to the inverse of the number of atoms (1/n) of silver clusters in Ag_n-Pz-Ag_n molecular junctions with d_{MM}=9.0 Å.

excitations of the bridge molecule which are absent in a single metal cluster.

To compute the ground and singlet excited states energies *Gaussian 09* implementation[8] of the long-range corrected M06-HF[9] functional in combination with the LanL2DZ[10] basis set has been used. This functional contains the full HF exchange and provides good estimations of the energies of CT states.[11] Excited state calculations has been restricted to the Frank-Condon (FC) point. Although some amount of charge is transferred between both metals or between the metals and the molecule in the ground and excited states, charge transfer states (CT) are easily recognized by checking the Mulliken's charges of the moieties and the CI expansion. The transferred charge in CT states usually lies in the range 0.6-0.9 a.u., while it is less than 0.10 a.u. in the remaining non-CT states.

Equilibrium ground state structures with D_{2h} symmetry have been found for all the investigated closed shell systems, with a distance between the two closest silver atoms of each cluster amounting to $d_{MM,eq}$≈7.5 Å. At the respective equilibrium geometries it is not possible to find electronic excited states with metal-to-metal CT character (CT_{MM}), due to the metallic molecular orbitals are symmetrically delocalized along both clusters under D_{2h}.

The effect of the inter-electrode distance (d_{MM}) on the electronic structure has been investigated by computing the respective optimized geometries and TD-DFT vertical energies in the range d_{MM}=7.0-11.0 Å in steps of 0.5 Å. It is found that for d_{MM} distances larger than 8.0 Å the symmetric D_{2h} structure is lost because Pz preferably links to one of the clusters (M_C: contact metal, M_{NC}: non-contact metal) giving a C_{2v} M_C-Pz…M_{NC} junction. When pyrazine is bonded and closer to one of the metals the electrodes become not equivalent. The interaction of the nonbonding electrons of the nitrogen with the bonded metal produces the injection of a small Mulliken´s charge amounting to 0.09-0.10 a.u. for n=2-8, respectively, in the contact cluster. This raises slightly the $HOMO_M$ (FL_C) of the metal to which the molecule is adsorbed (Fig. 1b) and the symmetry of the system is reduced to C_{2v}. This small charge transfer process in the ground electronic state of the systems corresponds to the charge transfer induced potential of Ratner *et al.*[12] The confinement of the metallic molecular orbitals inside each cluster allows for emerging localized metal-to-metal CT_{MM} electronic states.

Although the adsorption process is weak (M_C-A bond energy is only 0.5 eV, Fig. S1) it has important consequences in the electronic structure of Ag_n-Pz…Ag_n junctions as can be seen in Fig. 3. This Figure shows the linear dependence of the vertical energies of selected CT excited states of these systems at d_{MM}=9.0 Å on the inverse of the length of the chains (or the number of silver atoms, 1/n),[13] depending on whether the transferred electron comes from the contact (right panel) or the non-contact (left panel) metals.

CT_{MM} are excited states of the junction which can be electrified in the forward (CT_{MMF}:$HOMO_C$→$LUMO_{NC}$, M_C^+-A…M_{NC}^-) or reverse (CT_{MMR}:$HOMO_{NC}$→$LUMO_C$, M_C^--A…M_{NC}^+) directions (Figs. 1c and 1d) respectively. Metal-to-molecule CT states arise from electron transfer from the FL of the metal ($HOMO_M$) to vacant orbitals of the pyrazine (CT_0;B_1: $HOMO_M$→$LUMO_A$; CT_1;A_2: $HOMO_M$→$LUMO_A$+1, *etc.*) and are also labelled as forward or reverse, $CT_{0,1F}$ (M_C^+-A^-…M_{NC}) or $CT_{0,1R}$ (M_C-A^-…M_{NC}^+), depending on the M_C or M_{NC} cluster from which the electron is transferred, respectively. Molecule-to-metal CT processes are very energetic in silver-pyrazine systems and have not been discussed.

By comparing left and right panels it is concluded that forward and reverse CT processes are not equivalent at all what would allow for current rectification. Rectification is an important property of molecular junctions able to produce asymmetric currents when potentials of equal magnitude but opposite sign are applied.[2] The chemical adsorption enriches slightly the density of negative charge of the contact electrode what favours forward M_C→M_{NC} and M_C→A CT processes but blue-shifts the reverse $CT_{0,1R}$ states 0.5-1 eV with respect the forward ones. Moreover, only CT_{MM} states are depending on 1/n, with a larger slope in the case of CT_{MMR}, while $CT_{0,1}$ remain almost insensitive to the length of the chains as occurs with the first singlet excited state of Pz (A*, $S_{1,Pz}$;B_1) also shown in Fig. 3.

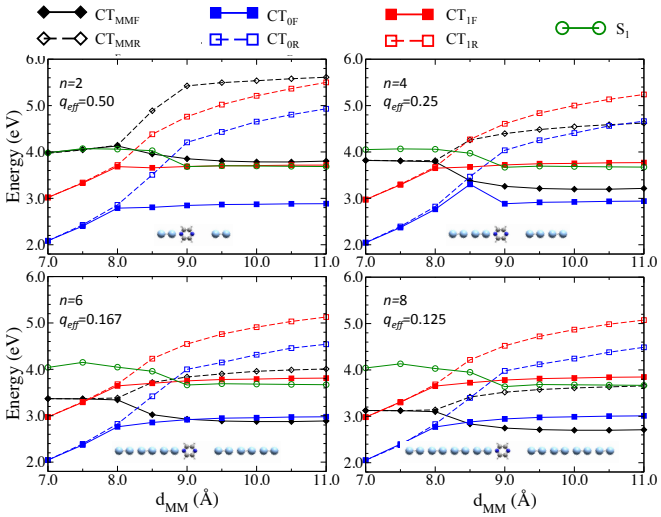

Fig. 4 Effect of the intercluster distance (d_{MM}) on the vertical energies of the CT_{MM}, CT_0 and CT_1,and $S_{1,Pz}$ electronic states of Ag_n-Pz-Ag_n. with n=2,4,6 and 8.

All the states in this Figure lie in the range 2.5-5.5 eV but their energies and relative positions depend also on d_{MM} as can be seen in Figs. 4 and S2 (ESI†). Two regions can be differentiated in these plots. All the states show degenerate energies for the respective forward and reverse processes in the compressed region at short distances d_{MM}≤8 Å where the weaker (M_CA)…M_{NC} bond is not significantly stretched near this critical value. This can be seen in Fig. S1 (ESI†) where the respective Ag_C-N_{Pz} and N_{Pz}-Ag_{NC} distances are represented *vs.* d_{MM}. Both bonds enlarge almost symmetrically until 8 Å, but once this critical point is overpassed, Ag_C-N_{Pz} bond is again shortened to its equilibrium distance (*ca.* 2.36 Å) while the N_{Pz}…Ag_{NC} distance progressively stretches, being the only recipient of additional Δd_{MM} increments.

CT_{MMF} and CT_{MMR} are not charged in the compressed region,[14] but forward and reverse branches appear differentiated in enlarged junctions (d_{MM}>8 Å) showing smaller splitting as the size of the chains increases (1.8 and 0.9 eV for n=2 and 8, respectively, in the range d_{MM}=9-11 Å). Concerning metal-molecule CT states, CT_1 is 1 eV above CT_0 in compressed junctions, where both are strongly stabilized *ca.* 0.8 eV (30%) when d_{MM} shortens from 9 to 7 Å. On the contrary, the energy of $S_{1,Pz}$ (*ca.* 3.7 eV) remains almost constant at large distances, irrespective of the size, but destabilizes slightly under compression (0.3-0.4 eV).

Forward and reverse CT_0 and CT_1 states also split in the enlarged region (d_{MM}>8-9 Å) mainly due to the respective reverse branches $CT_{0,1R}$;M_C-A^-…M_{NC}^+, whose energies increase as the positively charged donor cluster M_{NC}^+ is progressively moving away from the negatively charged acceptor M_CA^-. As expected, $CT_{0,1F}$ forward processes do not depend on the position of the neutral M_{NC} cluster at d_{MM}>8 Å given that is not involved in the $CT_{0,1F}$;M_C^+-A^-…M_{NC} electron transfer.

Standard conductance experiments in molecular junctions containing large metal electrodes are carried out under applied bias but charge transfer transport can be also induced by light excitation.[15] Analogously, the discussed CT_{MM} electrified states (M^+-A-M^-) can be taken as the starting point

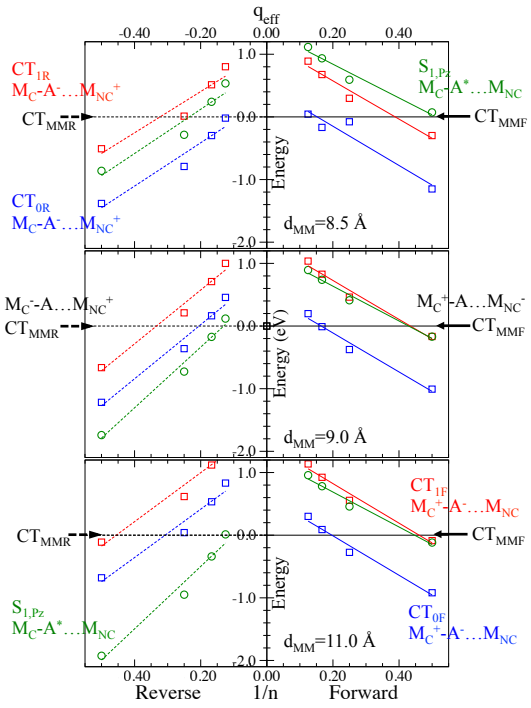

Fig. 5 Relative energies of metal-molecule $CT_{0,1}$ and molecular $S_{1;Pz}$ states referred to the energies of forward and reverse CT_{MM} states *versus* the inverse of the number of atoms (1/n, bottom) or the density of charge (q_{eff}=q/n, top) of the silver clusters in Ag_n^q-Pz-Ag_n^{-q} molecular junctions at d_{MM}=8.5, 9.0 and 11 Å.

for electron transport across these simple chain-like systems. In our models, CT_{MM} states can be reached, for instance, by photoexcitation, with very different energies for forward and reverse directions depending on both, 1/n and d_{MM}, as show Figs. 3 and 4:

$$S_0{:}M_C\text{-}A\ldots M_{NC} + h\nu \rightarrow CT_{MMF}{:}M_C^+\text{-}A\ldots M_{NC}^-$$

$$S_0{:}M_C\text{-}A\ldots M_{NC} + h\nu' \rightarrow CT_{MMR}{:}M_C^-\text{-}A\ldots M_{NC}^+$$

These polarized states act as energy reservoirs and can be taken as the origin of the energies for processes subsequent to electrization. CT_{MM} would play the role of the "injecting energy" in the "extended molecule" of Ratner *et* al.[4,16] corresponding to our Ag_n-A…Ag_n linear complexes.

Charge separation in CT_{MM} states can recombine through different mechanisms. Direct electronic transport across the junction is the opposite process where CT_{MM} decay to the S_0 ground state:

$$CT_{MMR}{:}M_C^-\text{-}A\ldots M_{NC}^+ \rightarrow S_0{:}M_C\text{-}A\ldots M_{NC}$$

$$CT_{MMF}{:}M_C^+\text{-}A\ldots M_{NC}^- \rightarrow S_0{:}M_C\text{-}A\ldots M_{NC}$$

Molecule mediated conduction produces enhanced electron transport and is allowed if metal-molecule $CT_{0,1}$ states lie below CT_{MM}. The fulfilment of this condition depends on both 1/n and d_{MM} and can be checked in Fig. 5. This Figure shows the relative energies of $CT_{0,1}$ and $S_{1,Pz}$ states in enlarged structures with d_{MM}=8.5, 9.0 and 11 Å with respect to the CT_{MMF} or CT_{MMR} states which are taken as the origin of the energies.

Fig. 5 shows that $CT_{0,1F}$ remain almost insensitive to the position of the M_{NC}^- donor group:

$$CT_{MMF}:M_C^+\text{-}A\ldots M_{NC}^- \rightarrow CT_{0,1F}:M_C^+\text{-}A^-\ldots M_{NC} \rightarrow S_0:M_C\text{-}A\ldots M_{NC}$$

But the reverse $CT_{0,1R}$ states stabilize 0.9-0.7 eV, respectively, when positively charged M_{NC}^+ approaches to the anionic A^- species:

$$CT_{MMR}:M_C^-\text{-}A\ldots M_{NC}^+ \rightarrow CT_{0,1R}:M_C\text{-}A^-\ldots M_{NC}^+ \rightarrow S_0:M_C\text{-}A\ldots M_{NC}$$

It can be see that the conduction channel through CT_0 is available in the case of forward polarization at any distance, except for n=8, while an equivalent situation is only found at short distances (d_{MM}=8.5 Å) when the sign of electrization is reversed.

Emission of electroluminescence from A* excited states of the molecule is also possible. Fig. 5 points out that $A^*:S_{1,Pz}$ is available at d_{MM}=8 or 9 Å from the more energy demanding CT_{MMR} polarization:

$$CT_{MMR}:M_C^-\text{-}A\ldots M_{NC}^+ \rightarrow S_{1,Pz}:M_C\text{-}A^*\ldots M_{NC} \rightarrow S_0:M_C\text{-}A\ldots M_{NC} + h\nu$$

This mechanism is not allowed in the forward panels of Fig. 5 because of the energy of $S_{1,Pz}$ always remains above CT_{MMF}.

Figs. 5 and S3 (ESI†) summarize the required conditions for each particular process and distance. The variable used in the x-axis (1/n, bottom) has been replaced by another one (q_{eff}, top) defined in the respective charged $CT_{MM}:M_C^q\text{-}A\ldots M_{NC}^{-q}$ excited states of the junctions, with forward (q=+1) and reverse (q=-1) polarizations, as:

$$q_{eff} = q_{eff,C} = -q_{eff,NC} = q/n$$

q_{eff} quantifies the average of the density of charge per atom in the CT_{MM} states of the respective Ag_n clusters and ranges from ±0.5 (n=2) to ±0.125 (n=8) a.u./silver atom. Therefore, the size of silver chains modulates the effective density of charge of the metal and, consequently, Fig. 5 can also be seen as showing the dependence of the relative energies of the $CT_{0,1}$ and $S_{1,Pz}$ states on q_{eff}, the charge density of the clusters. Electronic Supplementary Information (ESI) file contains the molecular orbitals involved in the discussed electronic states (Figs. S4-S7) and Table S1 summarizing single-electron excitations related to forward and reverse CT_{MM} and CT_0 charge transfer states.

q_{eff} (electron/atom) can be considered as a microscopic analogue of the macroscopic excess of surface charge of a metal (q', Coulomb/cm^2), which is controlled in a continuous way by the electric potential through the capacitance ($C=q'/E_V$). CT_{MM} states in these chain-like systems would be considered in turn as the microscopic analogue of a large molecular junction under applied electric potential, where the energy of the CT_{MM} state corresponds to the energy difference between the respective Fermi levels of the macro/microscopic electrodes ($E(CT_{MM}) \approx E(FL_{NC}) - E(FL_C) = eE_V$) (Figs. 1c and 1d).

Electron transport studies usually report statistical measurements using large electrodes where it is very difficult to control the experimental conditions at nanometer-size or atomic level. Conductance is controlled by the electronic structure of the overall junction, which is very sensitive to the particular geometry of the system. Concerning the metal, Gao et al.[17] have reported the strong dependence of the electronic excitations of silver clusters on the shape of the atomic chains. HOMO and LUMO energies of the metal can be tuned by geometric parameters of the cluster, but these frontier orbitals are involved in the metal-metal and metal-molecule CT states of the junction and therefore, the shape of the metal controls the energies of CT processes. Moreover, there is a general consensus on the critical role of the atomic-scale metal-molecule contact geometry and chemistry in the transport.[18] The presence of surface irregularities at these scales is unavoidable what implies geometrical uncertainties about the system to be modelled. Each particular adsorption site is characterized by an unknown nanometer/atomic density of charge which determines the line-up of the relevant electronic states as Fig. 5 shows. This introduces an almost unaffordable number of variables to be taken into account when modelling standard junctions containing large metals electrodes and complicates enormously any theoretical calculation. In these cases it is very difficult to include the effect of the bias and is almost unavoidable to discuss the results on the basis of molecular orbitals and metal levels (Fig. 1a) and does not on the stationary states of the overall system (Fig. 5). Although the obtained results for chain-like molecular bridges cannot be directly extrapolated to junctions with large metals they can be useful to understand the complex dependence of the electronic building on the electric potential. In this regard, Fig. 5 would show how the electronic structure of a standard junction is tuned by an applied bias able to induce a fractionary charge q_{eff} in the metal atom directly bonded to the molecule in the surface of a micro/macroscopic electrode.

This situation is very similar to that of surface-enhanced Raman scattering (SERS) which consists in the huge enhancement of the Raman signal of molecules on the surface of nanometer-size metal clusters.[19] SERS is a very complex phenomenon very dependent on the same factors above mentioned, particularly the electric potential of the interface. DFT calculations on metal-molecule systems including large metal clusters or slab models are very often used to support the discussion of both molecular junctions[2] or SERS results.[20] The likeness of a molecular junction and the proposed models for hot spots in SERS[21] prove the close relationship[22-25] between both kinds of experiments. We have previously shown the usefulness of DFT calculations in stick-like Ag_n^q-A complexes with different charges and sizes (n=3,5,7 with q=±1, n=2 with q=0) in order to model the effect of the electrode potential in SERS. These Ag_n^q-A charged systems are similar to the CT_{MM} states of the Ag_n-A…Ag_n junctions at infinite separation. We have shown that q_{eff} accounts for the experimental shifts observed in the SERS wavenumbers induced by the electrode potential.[26] It tunes linearly the CT states of the Ag_n^q-A complexes[27] and modifies smoothly the

relative intensities of the Raman bands.[28] This has allowed to detect resonant Raman processes involving CT metal-molecule (CT-SERS)[29] or plasmonic metal-metal (PL-SERS)[30] excited states in particular SERS, as well as to propose a comprehensive explanation for the unexpected effectiveness of the electrode potential in tuning the energy of the metal-molecule CT states.[31] Simple schemes like shown in Fig. 1a imply the equivalence between the applied bias (ΔE_V) and the corresponding shift of the energy of the CT states (ΔE_{CT}) ($G=\Delta E_{CT}/\Delta E_V=1$ eV/V)[32] but huge energy gains up to G=4-5 eV/V have been measured from SERS and others experiments.[31,33-35] On the basis of these simple chain-like models we have shown that the energy gain contains two different contributions G=SC. $C=q_{eff}/E_V$ is the electrical capacitance of the metal which quantifies its capability for converting the applied bias in surface excess of charge (q_{eff} in our model). $S=E_{CT}/q_{eff}$ is the dependence of the energy of each CT state on the surface charge q_{eff}. S is quantified through the slope of the particular state in Fig. 5. The gain is not uniform along the metal surface but is mainly located at large curvature sites[32] corresponding to hot spot in SERS or the tips of the electrodes in molecular junction devices. Therefore, it should be also relevant in conductance experiments and would invalidate any estimation of the required bias for molecule-mediated electron transport deduced from schemes like shown in Fig. 1.

Although the here reported DFT calculations must be taken as qualitative and restricted to atomic thickness junctions like those built by Ho *et al.*[4] they can be useful in order to understand the complex electronic structure of charged molecular junctions containing large metal electrodes. The non-equivalence between forward and reverse CT processes should be only significant in small metal clusters, but it could play a relevant role in some experiments using larger electrodes. Recent published works[36,37] discuss the formation of hybrid junctions where a single organic molecule is connected to chains of metal atoms like the here discussed formed at the end of large electrodes when the system is under tensile stress. It has been proposed that these hybrid junctions are a new type of atomic scale interfaces[38] and can be responsible for the anomalous enhancement of the conductance detected in particular experiments.[39]

Summarizing, on the basis of (TD)-DFT calculations the effect of the cluster size (n) and the distance between metals (d_{MM}) on the electronic structure of Ag_n-Pz-Ag_n chain-like molecular junctions has been investigated. The electronic structure shows a dual behaviour at short and large inter-cluster distances. In the last case, forward and reverse processes become non-equivalent due to the asymmetry induced by the adsorption of the molecule on one of the metals. As a result, a microscopic model to discuss the effect of the density of charge of the metal chains (q_{eff}) in the electronic states where the molecule is involved ($CT_{0,1}$ and $S_{1,Pz}$) has been proposed. It has been found that the relative energies of these electronic states depend linearly on the charge density of the metals, q_{eff}.

Financial support from MINECO (Grant CTQ2015-65816R) is gratefully acknowledged. FAF is a Juan de la Cierva fellow (IJCI-2014-21333). The authors thank SCAI and Rafael Larrosa of University of Malaga for computational resources and support.

Notes and references

1 A. Nitzan and M. A. Ratner, *Science*, 2003, **300**, 1384.
2 J. C. Cuevas and E. Scheer, *Molecular Electronics: An introduction to theory and experiment*, World Scientific, Singapore, 2010.
3 N. Nilius, T. Wallis and W. Ho, *Science*, 2002, **297**, 1853.
4 G. Nazin, X. Qiu and W. Ho, *Science*, 2003, **302**, 77.
5 D. R. Belcher, M. W. Radny, S. R. Schofield, P. V. Smith and O. Warschkow, *J. Am. Chem. Soc.,* 2012, **134**, 15312.
6 E. B. Guidez and Ch. M. Aikens, *Nanoscale*, 2012, **4**, 4190.
7 E. B. Guidez and Ch. M. Aikens, *Nanoscale*, 2014, **6**, 11512.
8 M. J. Frisch, *et al*., *Gaussian 09, Revission A.02*, 2009, Gaussian, Inc., and references therein.
9 Y. Zhao and D. G. Truhlar, *J. Phys. Chem. A*, 2006, **110**, 13126.
10 P. J. Hay and W. R. Wadt, *J. Chem. Phys.*, 1985, **82**, 270.
11 D. Jacquemin, E. A. Perpète, I. Ciofini, C. Adamo, R. Valero, Y. Zhao and D. G. Truhlar, *J. Chem. Theory Comput*., 2010, **6**, 2017.
12 Y. Q. Xue, M. A. Ratner, *Physical Review B*, 2003, **68**, 115406.
13 The particle in a box model predicts that the $HOMO_M$ energy of linear clusters with even number of atoms is not dependent on the size while the $LUMO_M$ energy is inversely proportional to the length of the chains.
14 CT_{MM} states at $d_{MM}\leq 8$ Å are degenerate and correspond to symmetric and antisymmetric combinations of the forward and reverse electrified configurations: $(M^+\text{-A-}M^-)\pm(M^-\text{-A-}M^+)$.
15 Z. Hu, M. A. Ratner and T. Seideman, *J. Chem. Phys.*, 2014, **141**, 224104.
16 S. N. Yaliraki, A. E. Robert, C. Gonzalez, V. Mujica and M. A. Ratner, *J. Chem. Phys.*, 1999, **111**, 6997.
17 B. Gao, K. Ruud and Y. Liu, *J. Phys. Chem. C*, 2014, **118**, 13059.
18 M. Di Ventra, S. T. Pantelides and N. D. Lang, *Phys. Rev. Lett.*, 2000, **84**, 979.
19 R. Aroca, *Surface-enhanced vibrational spectroscopy*, John Wiley & Sons Ltd., Chichester, 2006.
20 L. Jensen, Ch. M. Aikens and G. C. Schatz, *Chem. Soc. Rev.*, 2008, **37**, 1061 and references therein.
21 D. V. Chulhai, X. Chen and L. Jensen, *J. Phys. Chem. C*, 2016, in press DOI: 10.1021/acs.jpcc.6b02159,
22 M. Oren, M. Galperin and A. Nitzan, *Phys. Rev. B*, 2012, **85**, 115435.
23 T.-H. Park and M. Galperin, *Phys. Rev. B*, 2011, **84**, 075447.
24 F. Mirjani, J. M. Thijssen and M. A. Ratner, *J. Phys. Chem. C*, 2012, **116**, 23120.
25 Y. Li, P. Doak, L. Kronik, J. B. Neaton and D. Natelson, *Proc. Nat. Acad. Sci.*, 2014, **111**, 1282.
26 J. Soto, D. J. Fernández, S. P. Centeno, I. López Tocón and J. C. Otero, *Langmuir*, 2002, **18**, 3100.
27 F. Avila, D. J. Fernández, J. F. Arenas, J. C. Otero and Juan Soto, *Chem. Commun.*, 2011, **47**, 4210.
28 F. Avila, C. Ruano, I. López-Tocón, J. F. Arenas, J. Soto and J. C. Otero, *Chem. Commun.,* 2011, **47**, 4212.
29 S. P. Centeno, I. López-Tocón, J. Román-Pérez, J. F. Arenas, J. Soto and J. C. Otero, *J. Phys. Chem. C*, 2012, **116**, 23639.
30 J. Román-Pérez, I. López-Tocón, J. L. Castro, J. F. Arenas, J. Soto and J. C. Otero, *Phys. Chem. Chem. Phys.*, 2015, **17**, 2326.
31 J. Román-Pérez, C. Ruano, S. P. Centeno, I. López-Tocón, J. F. Arenas, J. Soto and J. C. Otero, *J. Phys. Chem. C*, 2014, **118**, 2718.

32 According to Fig. 1a, the applied bias E_V shifts symmetrically the FL's of both electrodes and therefore, the expected gain is G=1/2 eV/V.
33 L. Cui, D. W. Wu, A. Wang, B. Ren and Z. Q. Tian, *J. Phys. Chem. C*, 2010, **114**, 16588.
34 A. Otto, J. Billmann, J. Eickmans, U. Ertürk and C. Pettenkofer, *Surf. Sci.*, 1984, **138**, 319.
35 D. M. Kolb, *Angew. Chem., Int. Ed.*, 2001, **40**, 1162.
36 W. R. French, C. R. Iacovella, I. Rungger, A. M. Souza, S. Sanvito, and P. T. Cummings, *Nanoscale*, 2013, **5**, 3654.
37 A. Saffarzadeh, F. Demir and G. Kirczenow, *Phys. Rev. B*, 2014, **89**, 045431.
38 T. Yelin, R. Vardimon, N. Kuritz, R. Korytář, A. Bagrets, F. Evers, L. Kronik and O. Tal, *Nano Lett.*, 2013, **13**, 1956.
39 Ch. Bruot, J. Hihath and N. Tao, *Nat. Nanotechnol.,* 2012, **7**, 35.